Molecular Cloning and Characterization of Human *FGF8* Alternative Messenger RNA Forms[1]

Ananta K. Ghosh, Deepa B. Shankar, Gregory M. Shackleford, Kai Wu, Anne T'Ang, Gary J. Miller, Jianping Zheng, and Pradip Roy-Burman[2]

Departments of Pathology [A. K. G., A. T., J. Z., P. R-B.], Pediatrics [D. B. S., G. M. S., K. W., A. T.], and Molecular Microbiology and Immunology [D. B. S., G. M. S., K. W., A. T.], University of Southern California School of Medicine, Los Angeles, California 90033; Division of Hematology-Oncology, Children's Hospital of Los Angeles, Los Angeles, California 90027 [D. B. S., G. M. S., K. W., A. T.]; and Department of Pathology, University of Colorado Health Sciences Center, Denver, Colorado 80262 [G. J. M.]

Abstract

Three alternatively spliced mRNA isoforms of the human fibroblast growth factor-8 (*FGF8*) gene, expressed in a prostatic carcinoma cell line, have been isolated as cDNA clones and characterized by DNA sequencing. The clones, designated *FGF8*a, *FGF8*b, and *FGF8*e, differ from each other at the NH_2-terminal region of the mature proteins and share extensive nucleotide sequence homology in the protein coding region to the corresponding mouse cDNA isoforms that were previously reported. FGF8a and FGF8b exhibit identical amino acid sequences to those of their murine counterparts. *FGF8*e displays partial sequence variation from the corresponding mouse clone only in the extra exon sequence found in this isoform in both species. There is extensive sequence diversity between *FGF8* (human) and *Fgf8* (murine) genes in the 3′-untranslated region of the mRNAs. Northern blot analyses revealed *FGF8* mRNA expression only in fetal kidney tissue among the various fetal and adult human tissues tested. The reverse transcription-PCR amplification method, however, detected *FGF8* mRNA expression in adult prostate, kidney, and testes (the tissues that were tested) and in all normal and tumor prostatic epithelial cell lines examined; although expression of both *FGF8*a and *FGF8*b was seen in kidney and testes, *FGF8*b appeared to be the predominantly expressed species in the prostatic tissue and cell lines analyzed by reverse transcription-PCR. To address the biological effect of specific isoform expression, NIH3T3 cells were transfected with a eukaryotic expression vector containing cDNA for *FGF8*a, *FGF8*b, or *FGF8*e. Consistent with previous reports on differences in the transforming potential of mouse FGF8 isoforms, human FGF8b was found to induce marked morphological transformation to NIH3T3 cells and strong tumorigenicity of the transfected cells in nude mice. Human FGF8a and FGF8e were moderately transforming in NIH3T3 cells, and the transfected cells were moderately tumorigenic *in vivo*. These results document the production of three alternatively spliced *FGF8* mRNAs in human tissues and the transforming and tumorigenic potential of their protein products. Moreover, these data, combined with the tissue-specific expression of these isoforms, suggest that they may have different biological functions.

Introduction

The FGF[3] family represents a group of physiological signaling molecules that elicit their effects via high-affinity receptor tyrosine kinases (1, 2). The functional properties of most of these growth factors pertain to wound healing and embryonic development *in vivo* and mitogenic stimulation in a variety of cell types *in vitro* (3). Of the nine known members of this growth factor family (FGF1–FGF9), FGF8 was originally identified as AIGF because it mediated the androgen-dependent growth of a mouse mammary tumor cell line, SC-3 (4). Subsequent studies with the mouse *Fgf8* gene and its protein products have generated additional interest in the function of this gene. For example, there is evidence for a specific interaction of FGF8 with certain isoforms of FGF receptors (5), occurrence of a complex alternative splicing phenomenon that generates transcripts with coding potential for multiple secreted FGF8 proteins varying in their NH_2-termini (4–7), and differential cell transformation and tumorigenicity exhibited by these particular isoforms (8–10). Additionally, a strong collaboration between *Fgf8* and the *Wnt1* proto-oncogene in murine mammary tumorigenesis has been described (6).

Since androgen plays a profound role in prostatic epithelium and in regulation of androgen-dependent prostate cancers (11–13), we became interested in studying the human *FGF8* gene and its protein products in relation to their normal expression and potential abnormal regulation in the development of androgen-independent prostate cancers (14). To initiate this line of investigation, we describe here molecular

Received 6/4/96; revised 7/1/96; accepted 7/31/96.
The costs of publication of this article were defrayed in part by the payment of page charges. This article must therefore be hereby marked *advertisement* in accordance with 18 U.S.C. Section 1734 solely to indicate this fact.
[1] This work was supported by NIH Grant CA59705 and in part by NIH Grant CA58412, a grant from T. J. Martell Foundation, University of Colorado Cancer Center, NIH Grant CA46934 through the Cytogenetics Core Laboratory, University of California Breast Cancer Research Program Grant 1RB-0484, a postdoctoral fellowship from NIH Training Grant T32-CA09320, and predoctoral fellowship DAMD 17-94-J-4319 from the Department of the Army.
[2] To whom requests for reprints should be addressed, at Department of Pathology, University of Southern California School of Medicine, 2011 Zonal Avenue, Los Angeles CA 90033.

[3] The abbreviations used are: FGF, fibroblast growth factor; AIGF, androgen-induced growth factor; RT, reverse transcription; RACE, rapid amplification of cDNA ends; poly(A)$^+$ RNA, polyadenylated RNA; FBS, fetal bovine serum; GAPDH, glyceraldehyde-3-phosphate dehydrogenase.

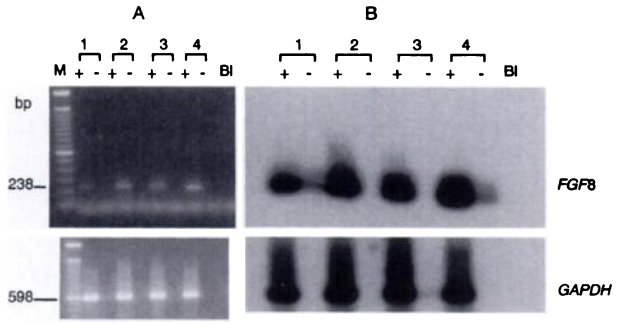

Fig. 1. Detection of *FGF8* mRNA in prostatic epithelial tumor cell lines by RT-PCR. *Columns 1–4*, LNCaP, PC-3, DU145, and ALVA-31 cell lines, respectively. Each *column* has two *lanes*, one showing PCR amplication after RT (+), and the other without RT (−). *A*, ethidium bromide staining of gels indicating bands corresponding to size fragments of *FGF8* and *GAPDH*. *B*, Southern blot of the same gel using either murine *Fgf8* cDNA or human *GAPDH* cDNA as probe. *Bl*, blank reaction.

cloning of human *FGF8* cDNA sequences from a prostate carcinoma cell line, identification of cDNAs encoding three protein isoforms, and the expression pattern of this gene in various prostate epithelial cell lines and in adult and embryonic human tissues. Furthermore, we present evidence that like mouse FGF8 isoforms, human homologues have differential abilities to induce morphological transformation of NIH3T3 cells *in vitro*, and their tumorigenicity *in vivo*.

Results

Isolation of Human *FGF8* cDNA Isoforms and Their Sequence. Initially we determined whether mRNA homologous to murine *Fgf8* is expressed in prostate epithelial cell lines using the RT-PCR amplification method. With two primers specific for the *Fgf8* exon 5 sequence (4), we obtained a single prominent amplified product of expected 238 bp from the mRNAs of each of the four human prostatic carcinoma cell lines LNCaP, PC-3, DU145, and ALVA-31 (Fig. 1). Of these, the DU145 cell line was selected to amplify the full coding sequence of the human message corresponding to *Fgf8* using PCR primers that represented the 5′- and 3′-termini of the published murine coding sequence (4). Analysis of the cloned cDNA products derived from DU145 cells revealed alternatively spliced mRNAs encoding three different FGF8 isoforms: FGF8a, FGF8b, and FGF8e (Figs. 2 and 3). As seen in the deduced amino acid sequence (Fig. 3), all isoforms carry the same predicted signal peptide sequence and the same protein sequence downstream of the alternative splice point. The isoforms differ in the length of the amino acid sequence retained in the amino-terminal regions. The extent of nucleotide sequence homology between *Fgf8* and *FGF8* cDNAs indicates a high level of sequence conservation of the gene between mammalian species. For example, comparison of the nucleotide sequence of human *FGF8b* shown in Fig. 2 with that type of isoform of mouse (*Fgf8b*) showed a difference of only 29 nucleotides within the 648-nucleotide coding region (95.5% homology). Amino acid homology is further striking as it is identical in murine FGF8 and human FGF8 when isoforms a and b are considered (4, 6). A previous study of an exon-containing fragment of the human *FGF8* gene revealed a 100% identity to amino acids 85–120 of the mouse *Fgf8* (10). A more recent report (15), which appeared during the course of our work, also described complete identity in amino acid sequence of human and mouse FGF8b isoform. We did not obtain a cDNA corresponding to mouse FGF8c (6) but did isolate another version that we named FGF8e and that is homologous to one of the variants (variant 7) cloned from mouse embryos (7). The deduced peptide sequence of the additional exon of FGF8e differs from the mouse sequence of variant 7 at 4 of the 29 amino acid positions as shown in Fig. 3. The remainder of the 233-amino acid FGF8e coding domain is identical to the amino acid sequence of mouse FGF8 clone 7, indicating an overall homology of 98.3%.

The 3′-untranslated region was cloned from DU145 poly(A)$^+$ RNA by the RACE procedure. The appropriately derived PCR product was cloned into the TA cloning vector and analyzed for its DNA sequence. There is extensive diversity between mouse and human *FGF8* gene sequences in the 3′-untranslated portion examined (Fig. 4). We confirmed the contiguousness of this human sequence to the *FGF8* coding sequences by designing PCR primers at this region and using them in pairs with other primers located in the coding region. PCR products were always obtained in which the sequence corresponded to natural juxtaposition of the 3′-untranslated portion to the protein coding sequence of *FGF8* cDNA.

Expression of *FGF8* in Human Tissues. We conducted Northern blot analysis of poly(A)$^+$ RNA from several normal human tissues to examine the expression patterns of *FGF8*. Northern blots were hybridized first to ^{32}P-labeled *FGF8* cDNA, and then, after exposure and stripping of the probe, hybridized again to ^{32}P-labeled human β-actin. As shown in Fig. 5, only fetal kidney displayed a detectable level of *FGF8* mRNA, whereas other fetal tissues (*e.g.*, brain, lung, and liver) tested negative. All adult tissues tested (spleen, thymus, prostate, testes, ovary, small intestine, colon, and peripheral blood lymphocytes) did not produce sufficient amounts of *FGF8* mRNAs to be detected by Northern blot analysis. High expression of *Fgf8* has been reported in mouse embryos of early gestational age that diminished to nearly undetectable levels by 14.5 days postconception (6, 10). Since gestational age of the human fetuses used in the preparation of the commercial blots is unknown, lack of detectable expression of *FGF8* gene in the fetal brain, lung, and liver tissues was not surprising. Although the strong expression in fetal kidney is noteworthy, its significance is not known at this time. Regarding adult human tissues, we expected to find expression of *FGF8* in ovary and testes since these were the only two adult mouse tissues in which expression was previously reported in one study (6). Another report described detection of a low level of expression of *FGF8* by Northern blot in adult mouse testes (10). However, no expression was detected in these two human tissues by Northern blotting. It is possible that an inbred mouse line may indeed be different from the outbred human species in *FGF8* expression patterns, or the difference may be a matter of sensitivity between the previous experiments (6, 10) and this

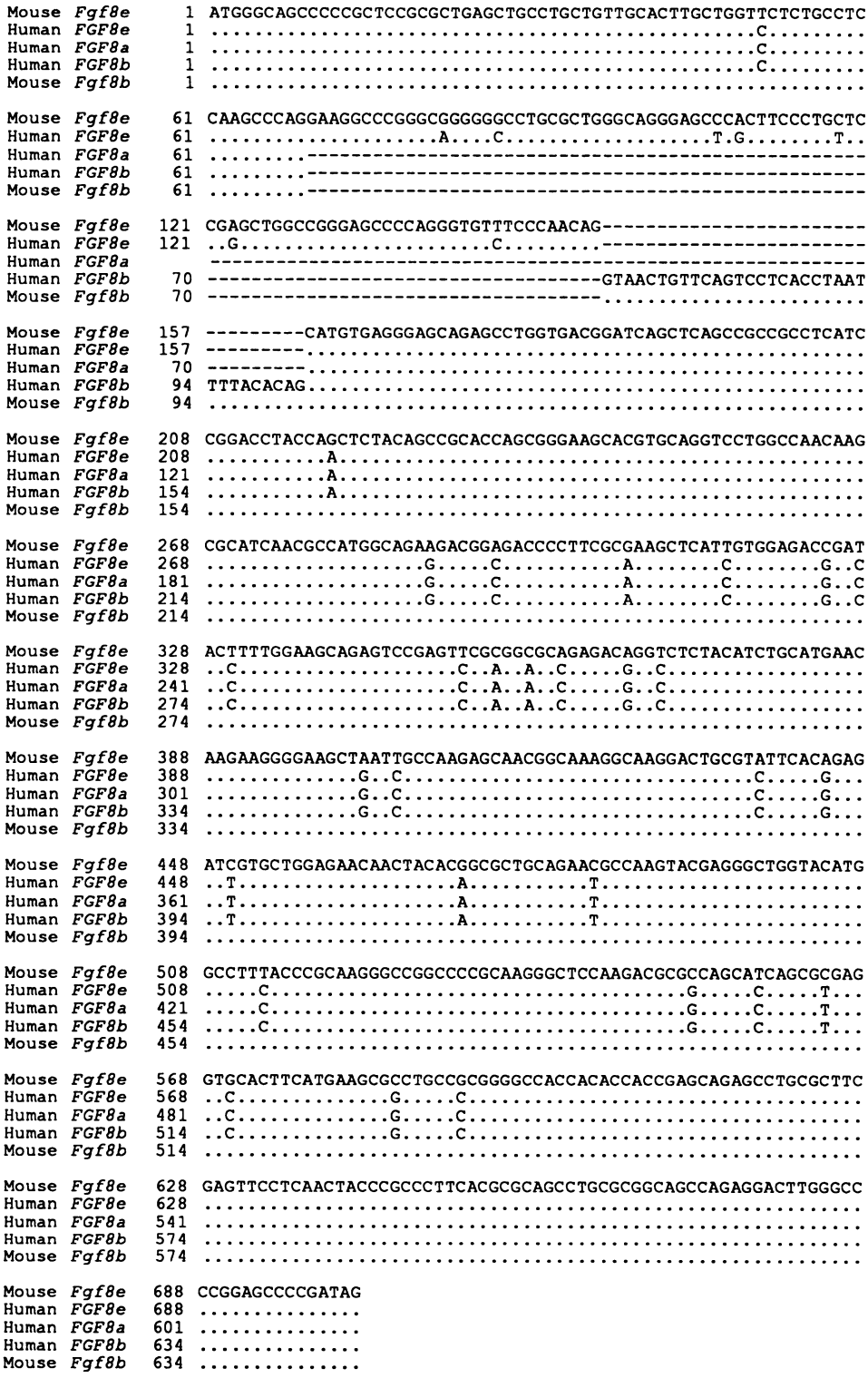

Fig. 2. Nucleotide sequences of the human *FGF8* cDNA isoforms. The nucleotide sequence starts at the beginning of the coding region and extends to the termination codon. The sequence of the mouse *Fgf8* previously reported as AIGF1 (4) or *Fgf8*b (6) and that of *Fgf8* variant 7 (7), which we named *Fgf8*e, are shown, and the identical nucleotides in the sequences of the human isoforms are indicated by *dots*. Sequence gaps, denoted by *dashes*, mark the alternatively spliced forms.

study. With use of a more sensitive method (RT-PCR), we detected expression of *FGF8* in adult human testes as well as in prostate and kidney tissues (Fig. 6). In this experiment, a primer set was used that yielded products that could be readily resolved to indicate isoform-specific expression patterns. Although *FGF8*b was the predominant isoform in the prostate, testes and kidney tissues showed expression of both *FGF8*a and *FGF8*b products. Similar to the prostate tissue pattern, prostate-derived normal epithelial cell line (MLC SV40$^-$) and carcinoma cell lines (LNCaP, ALVA-31,

```
Mouse FGF8e     1 MGSPRSALSCLLLHLLVLCLQAQEGPGGGPALGREPTSLLRAGREPQGVS
Human FGF8e     1 ........................R.......LA..F..........
Human FGF8a     1 ........................-------------------------
Human FGF8b     1 ........................-------------------------
Mouse FGF8b     1 ........................-------------------------

Mouse FGF8e    51 QQ-----------HVREQSLVTDQLSRRLIRTYQLYSRTSGKHVQVLANK
Human FGF8e    51 ..-----------.....................................
Human FGF8a    24 -------------.....................................
Human FGF8b    24 --VTVQSSPNFTQ.....................................
Mouse FGF8b    24 --.....................................................

Mouse FGF8e    90 RINAMAEDGDPFAKLIVETDTFGSRVRVRGAETGLYICMNKKGKLIAKSN
Human FGF8e    90 .....................................................
Human FGF8a    61 .....................................................
Human FGF8b    72 .....................................................
Mouse FGF8b    72 .....................................................

Mouse FGF8e   140 GKGKDCVFTEIVLENNYTALQNAKYEGWYMAFTRKGRPRKGSKTRQHQRE
Human FGF8e   140 .....................................................
Human FGF8a   111 .....................................................
Human FGF8b   122 .....................................................
Mouse FGF8b   122 .....................................................

Mouse FGF8e   190 VHFMKRLPRGHHTTEQSLRFEFLNYPPFTRSLRGSQRTWAPEPR
Human FGF8e   190 ........................................
Human FGF8a   161 ........................................
Human FGF8b   172 ........................................
Mouse FGF8b   172 ........................................
```

Fig. 3. Comparison of the deduced amino acid sequences of the three human *FGF8* cDNA isoforms with those of mouse *Fgf8* isoforms. The mouse isoforms correspond to the original isolate AIGF1 (4) or *Fgf8*b (6) and *Fgf8*e (7). Identical amino acids are indicated by *dots*. Note that following the predicted signal peptide sequence (positions 1–23), the three isoforms differ only at the amino termini of the secreted forms. *Dashes*, sequence gaps.

```
Mouse Fgf8     1 -GCGCTCGCCCAGCTCCTCCCCACCCAGCCGG-CCGAGGAA---------
Human FGF8     1 G.A...-...TG..-.........AAT...A.A...CA..GAGGCTCATC

Mouse Fgf8    40 ------------------TCCAGC---GGGAGCTCGGCG--GCACAGCAA
Human FGF8    49 CTGTAGGGCACCCAAAAC..A..GCTG.......GT...CT..T.T...G

Mouse Fgf8    68 A--GGGGAGGGGCTGGGG-AGC--TGCCTTCTAGTTGTGCATATTGTTTG
Human FGF8    99 GCT.......T.......G...CC..GG...CG.....TG......
```

Fig. 4. Sequence diversity between *FGF8* and *Fgf8* cDNAs in the 3′-untranslated region. Nucleotide identity is indicated by *dots* and gaps by *dashes*. Nucleotide position 1 marks the first nucleotide immediately after the TAG termination codon. The mouse sequence represents nucleotide positions 823–984, as reported by Tanaka *et al.* (4).

PC-3, and DU145) all revealed over-representation of the *FGF8*b isoform. Since cDNA isoforms of *FGF8*a and FGF8e were indeed cloned from the DU145 cell line, the presence of these expressed isoforms appeared to be minor compared to *FGF8*b expression in these prostatic epithelial cell lines.

Morphological Transformation of NIH3T3 Cells Induced by Expression of FGF. The three *FGF8* isoform cDNAs were subcloned into the mammalian expression vector pcDNA3. The vectors, with inserts in either the sense or antisense orientation, along with the vector-only control, were used to transfect NIH3T3 cells. Stable transfectants were selected with G418. Pooled G418-resistant cells rather than individual clones were examined to avoid potential atypical representation due to clonal variation. Of all the different isolates of transfected NIH3T3 cells, the cells transfected with *FGF8*b cDNA in the sense orientation displayed the most striking phenotypic changes (Fig. 7). These cells exhibited marked morphological transformation with an elongated, spindle-like shape, in contrast to the generally flat morphology seen with control transfectants receiving the vector alone or an *FGF8*b antisense construct. They also grew to a higher cell density at confluence than did control cultures, indicating a loss of contact inhibition. NIH3T3 cells transfected with the FGF8a and FGF8e cDNAs were less strongly morphologically transformed than those cells receiving FGF8b and were roughly equal in phenotype to each other. The cells of these two pools were detectably more refractile by phase contrast microscopy and produced more processes than controls (Fig. 7). Like the FGF8b-transfected cells, the cells expressing FGF8a and FGF8e demonstrated loss of contact inhibition at confluence. These results corresponded closely to those described previously for mouse FGF8 isoforms (8, 9). Since the deduced amino acid sequence of FGF8b is identical between mouse and human, it was not surprising to find that human FGF8b, like mouse FGF8b when expressed from the corresponding cDNA, could induce morphological transformation to NIH3T3 cells. Similarly, the result that cells transfected with human *FGF8*a cDNA could not exhibit strong morphological transformation was consistent again with its amino acid sequence homology to the mouse *Fgf8*a isoform. Additionally, our results indicate that another isoform, *FGF8*e, which has a sequence domain partially specific for the human protein, also possesses a modest transforming function. The fact that these three

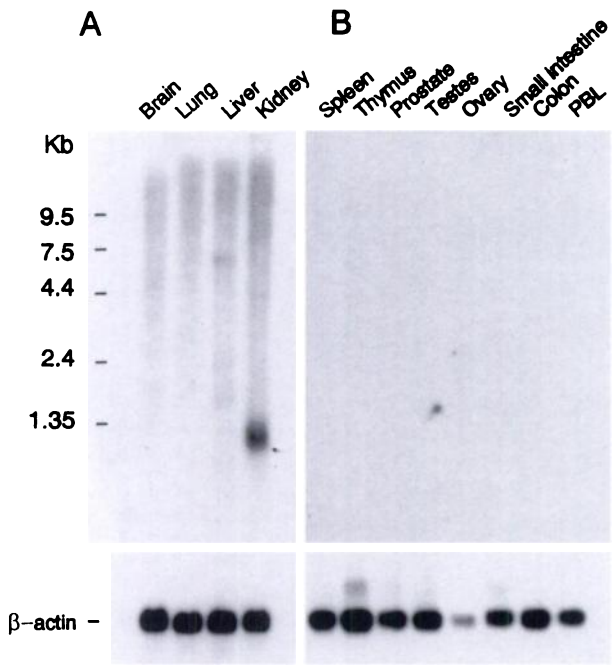

Fig. 5. Detection of *FGF8* expression in the fetal kidney tissue. Northern blots of normal adult and fetal tissue poly(A)$^+$ RNAs were probed with either *FGF8* cDNA or human β-actin cDNA. *A*, fetal tissues (brain, lung, liver, and kidney); *B*, adult tissues (spleen, thymus, prostate, testes, ovary, small intestine, colon, and peripheral blood lymphocytes). The blot was initially probed with *FGF8*b cDNA (*top panel*), and then with β-actin cDNA (*bottom panel*). The locations of RNA size markers for the top panels are shown at left.

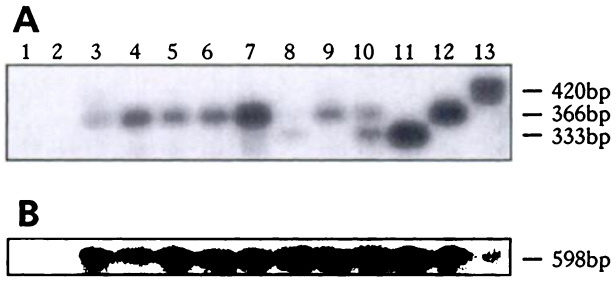

Fig. 6. Detection of *FGF8* mRNA isoforms by RT-PCR. Poly(A)$^+$ RNA from prostate epithelial cell lines and human tissues and total RNA from *FGF8* isoform-transfected NIH3T3 cell lines were examined by RT-PCR using the RB416 and RB418 primer pair. Although all analyses were conducted with and without RT, the negative results obtained when RT was not used are only illustrated in *Lanes 1* (MLC SV40 cells) and *2* (LNCaP cells). Other lanes (with RT): *Lane 3*, MLC SV40 ; *Lane 4*, ALVA-31; *Lane 5*, PC-3; *Lane 6*, DU145; *Lane 7*, LNCaP; *Lane 8, human adult kidney; Lane 9*, human adult prostate; *Lane 10*, human adult testes; *Lane 11*, NIH3T3 cells transfected with *FGF8*a; *Lane 12*, NIH3T3 cells transfected with *FGF8*b; and *Lane 13*, NIH3T3 cells transfected with *FGF8*e. After electrophoresis, the blot was hybridized first to ^{32}P end-labeled RB402 oligonucleotide (*A*), and then to human *GAPDH* cDNA probe (*B*).

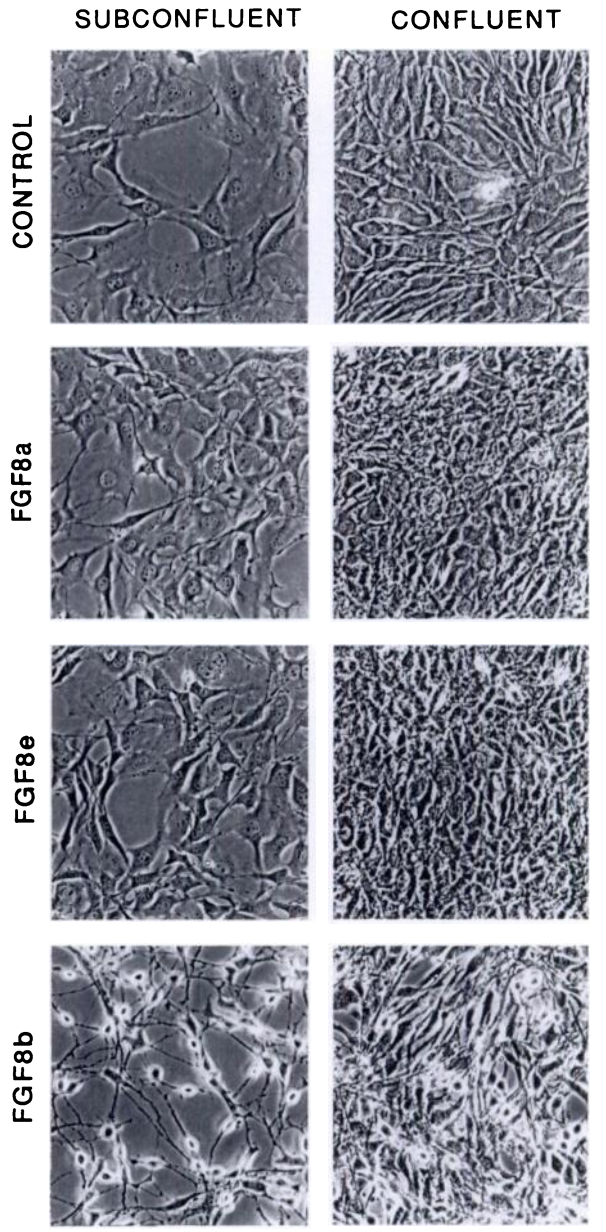

Fig. 7. Representative illustrations of morphological transformation of NIH3T3 cells by FGF8 isoforms. In this experiment, NIH3T3 cells were transfected with expression plasmids containing cDNAs of *FGF8*a, *FGF8*b, *FGF8*e, or a control plasmid with no insert. G418-resistant colonies were pooled and grown for examination of induced changes in morphology and contact inhibition. *FGF8*b showed strong morphological transforming ability, and *FGF8*a and *FGF8*e showed moderate transforming activity. All three isoforms induced a loss of contact inhibition at confluence.

FGF8 isoforms are secreted from the cells was demonstrated by a biological assay, which, however, was by nature not quantitative. NIH3T3 cells transfected with the plasmid vector could be strongly transformed by exposure to conditioned medium from *FGF8*b-transfected cells. Similarly, conditioned medium from *FGF8*a- and *FGF8*e-transfected cells induced morphological changes, although exhibiting a lower level of transformation. These results, not shown, closely resembled the findings described in Fig. 7.

Tumorigenicity Studies with Transfected NIH3T3 cells. The tumorigenicity of NIH3T3 cells transfected with different *FGF8* cDNA isoforms was examined by intraocular inoculation of the transfected cells into the anterior chamber of the

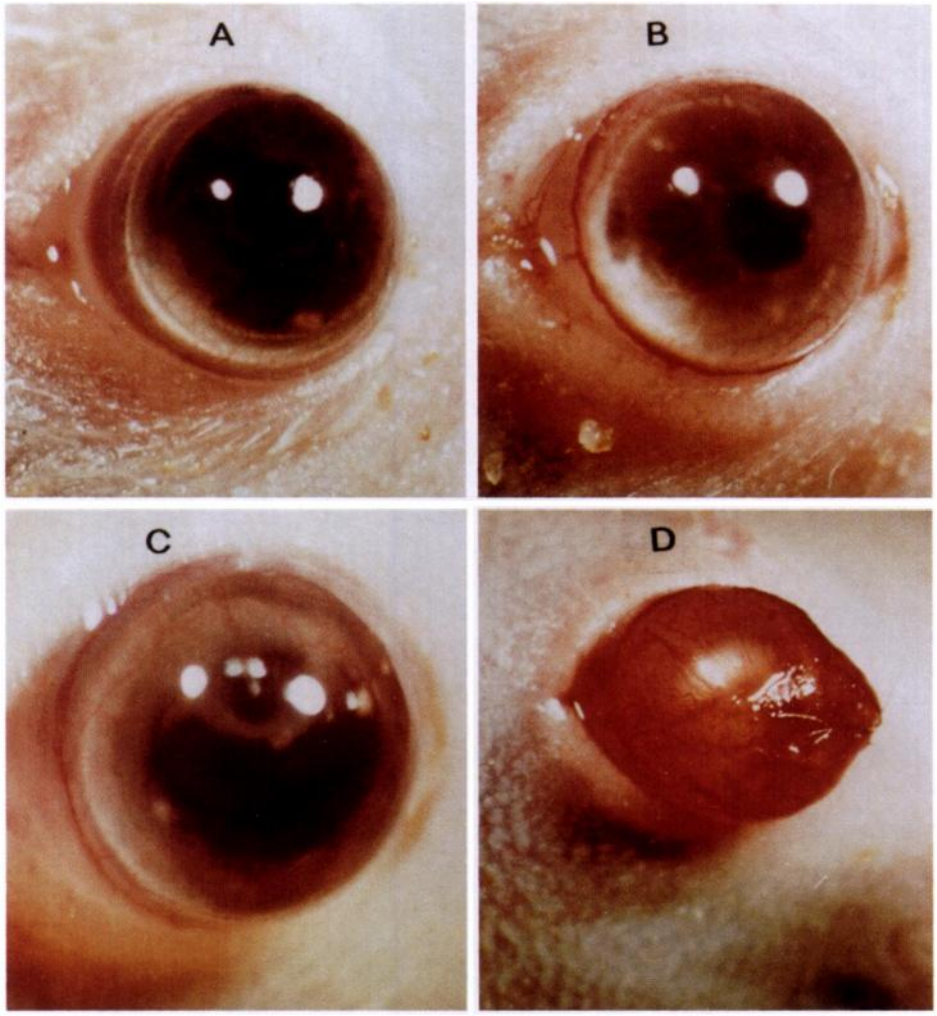

Fig. 8. Rapid tumorigenesis of *FGF*8b-transfected NIH3T3 cells. Cells (10^3) transfected with vector alone (*A*), *FGF*8a (*B*), *FGF*8e (*C*), or *FGF*8b (*D*) were injected intraocularly and the pictures taken at 12 days postinjection. While tumors were produced by *FGF*8b-transfected cells, cells transfected with other two isoforms grew better than the vector alone transfected cells as apparent from increased cloudiness in (*B*) and (*C*) relative to (*A*).

eye of nude mice. An advantage of the analysis, in addition to the sensitivity of the method, is that the cell growth and tumor formation can be readily monitored under the microscope (16, 17). As illustrated in Figs. 8 and 9, *FGF*8b-transfected cells demonstrated the ability to grow rapidly and produce tumors that ruptured the eye. Such vigorous tumor formation was not observed with cells transfected with either *FGF*8a or *FGF*8e, although all cells, including the vector-transfected NIH3T3 cells, could proliferate *in vivo* in the orbital fluid (Fig. 9), and after a longer latency, both *FGF*8a- and *FGF*8e-transfected cells could also produce tumors in several animals. As summarized in Table 1, as few as 10^2 *FGF*8b-transfected cells consistently produced tumors within 18–20 days when injected intraocularly; inoculation of a larger number of cells (10^3 or 10^4) led to formation of tumors even earlier. Although no tumors could be observed with 10^2-10^4 cells transfected with the vector alone during the 11 weeks of observation, all of the animals injected with 10^4 cells transfected with either *FGF*8a or *FGF*8e developed tumors similar to that induced by *FGF*8b (Fig. 8) after a latency of 6–8 weeks. Two of three animals receiving 10^3 cells of *FGF*8a-NIH3T3 cells and one of three receiving 10^2 of these cells developed tumors over a period of 6–10 weeks, whereas animals receiving 10^2 or 10^3 *FGF*8e-NIH3T3 cells did not exhibit tumors during the 11 weeks of observation.

Tumors were isolated from two animals that received *FGF*8b-transfected cells. From another animal that received only vector-transfected cells, *in vivo* propagated cells were collected and G418-resistant cells were reselected in culture. Northern blot analyses of RNA of 0.8 kb (which was expected from the design of the expression vector) from these tissues and cultured cells show that *FGF*8 RNA was present in the tumors but not in the control cells (Fig. 10). These results suggest the expression of the transfected genes is stable and is not altered by *in vivo* propagation in nude mice.

Lack of *FGF*8 Gene Induction by Androgen in LNCaP Cells. LNCaP, the only prostate carcinoma cell line known to be responsive to androgen, was investigated for stimulation of *FGF*8 expression after exposure to dihydrotestosterone. A 3–5-fold increase in cell proliferation was recorded relative to unstimulated LNCaP cells over a period of 72 h of exposure. However, there was apparently no significant change in the expression of *FGF*8 mRNA at various time points following androgen exposure. Although the detection

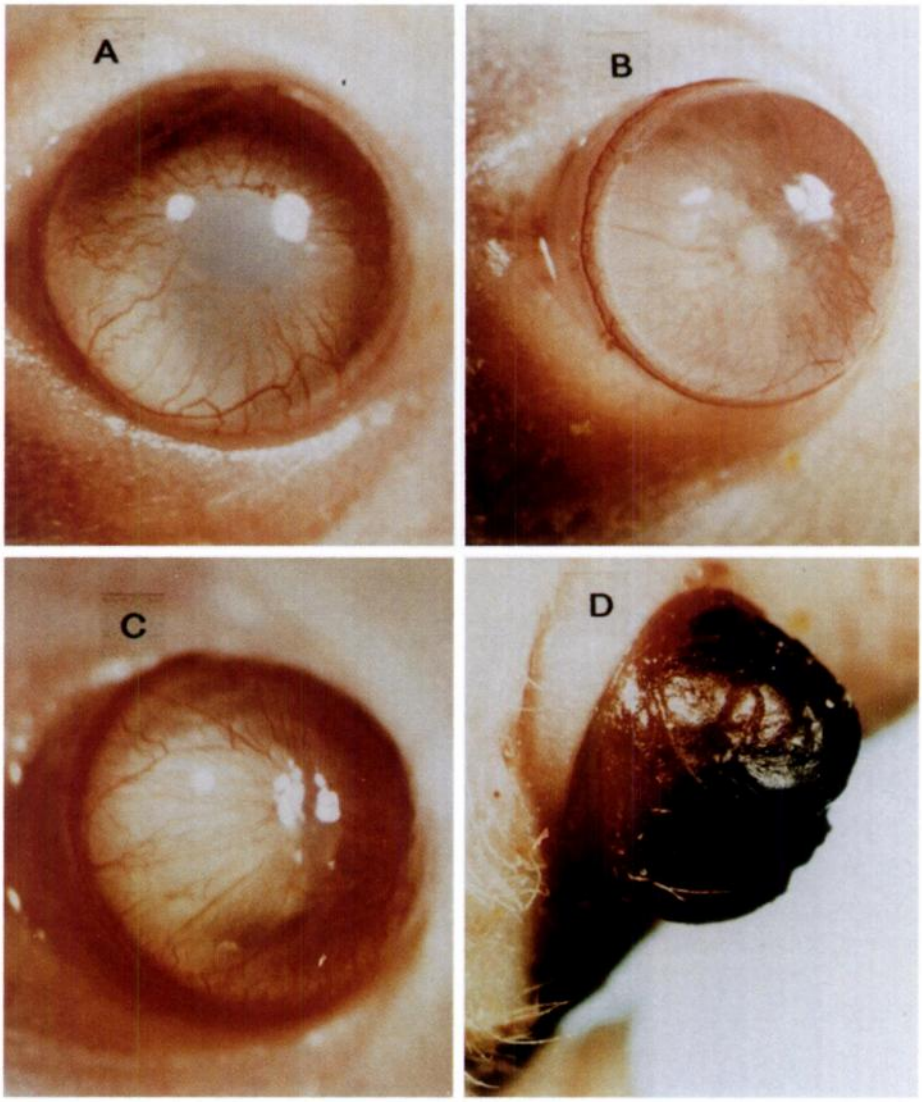

Fig. 9. Growth of transfected cells in the mouse eye. Cells (10^4) transfected with vector alone (*A*), *FGF*8a (*B*), *FGF*8e (*C*), or *FGF*8b (*D*) were injected intraocularly; the pictures were taken at 10 days postinjection. While all injected cells grew intraocularly, only *FGF*8b-transfected cells produced tumors consistently at this early time point.

method was based on RT-PCR analysis that did not permit a precise quantitative comparison, repeated analysis of several independent experiments conducted along with *GADPH* RT-PCR as an internal control did not reveal a significant alteration in *FGF*8 expression in this cell line in response to androgen exposure. An example of such analysis is illustrated in Fig. 11.

Discussion

In recent studies, mouse *Fgf*8 mRNAs were characterized as products of alternative splicing in the 5′ region of the gene. Initially, Tanaka *et al.* (4) reported two isoforms induced by androgen in a mouse mammary carcinoma cell line. Subsequently, three cDNA isoforms were isolated by MacArthur *et al.* (6), two of which (*Fgf*8b and *Fgf*8c) were identical to AIGF1 and AIGF2 (4), respectively; the third one was named as *Fgf*8a. Finally, four additional *Fgf*8 RNAs encoding different protein isoforms were reported by Crossley and Martin (7). All of these different isoforms appear to be derivatives of differ-

Table 1 Tumorigenicity of NIH3T3 cell lines expressing *FGF*8 isoform cDNAs

Cell line transfected with	No. of cells injected	Tumorigenicity	Tumor latency
*FGF*8a[a]	10^2	1/3	10 weeks
	10^3	3/3	6–8 weeks
	10^4	3/3	6–8 weeks
*FGF*8b[b]	10^2	6/6	18–20 days
	10^3	6/6	10–12 days
	10^4	6/6	7–8 days
*FGF*8e[a]	10^2	0/3	
	10^3	0/3	
	10^4	3/3	6–8 weeks
Vector alone[a]	10^2	0/3	
	10^3	0/3	
	10^4	0/3	

[a] Results shown were obtained from the second experiment with a longer period of observation (up to 11 weeks). In the first experiment, also, three animals were used for each set of injection, but no tumors developed during the 4 weeks of observation, at which time the experiment was terminated.

[b] Combined results of first and second experiments.

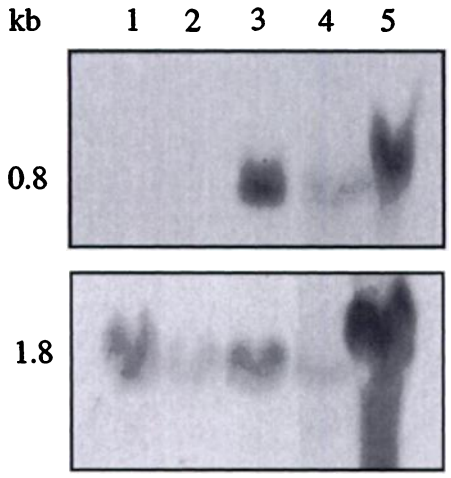

Fig. 10. Detection of *FGF8*b expression in tumors induced by *FGF8*b-transfected NIH3T3 cells. The total cellular RNA was subjected to Northern blot analyses with a ^{32}P-labeled *FGF8*b cDNA probe (*top panel*). *Lane 1*, vector alone transfected cells; *Lane 2*, vector alone transfected cells after propagation in mouse eye; *Lane 3*, *FGF8*b-transfected cells; and *Lanes 4* and *5*, two tumors produced by *FGF8*b-transfected cells. *Bottom panel*, analysis of the same blot with ^{32}P-labeled human actin cDNA.

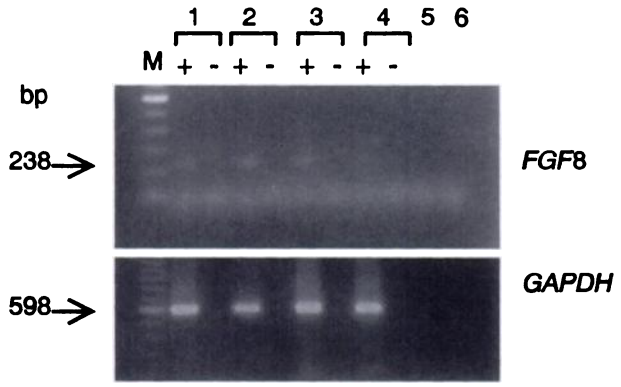

Fig. 11. Analysis of *FGF8* mRNA expression in androgen-stimulated LNCaP prostate tumor cell line. *Lane 1*, unstimulated cells; *Lanes 2–4*, stimulated cells at 8, 24, and 72 h postexposure to 10^{-8} M dihydrotestosterone, respectively; *Lane 5*, RT control (without RNA); and *Lane 6*, water control. Each lane shows RT-PCR products with (+) or without (−) RT. DNA markers (*M*) of 100-bp ladder and positions of expected *FGF8* and *GAPDH* products are also indicated.

ential exon usage and differential involvement of splice donor and acceptor sites within these exons (5–7). The products retain a common large COOH-terminal portion and vary in only a short domain residing between the signal peptide and the beginning of the conserved FGF core sequence (6, 7).

In this report, we describe the isolation of three distinct cDNAs of human *FGF8* expressed in a prostatic carcinoma cell line. Two of these cDNA isoforms are highly homologous to murine AIGF1 (or *Fgf*8b) and *Fgf*8a in terms of nucleotide sequence of the coding region and identical to them in the deduced amino acid sequence. These results are in agreement with the recent reports that there is 100% amino acid identity between a fragment of the human gene sequenced and that of mouse *FgF8* gene amino acids 85–120 (10), and there is complete deduced amino acid homology between human and mouse FGF8b isoforms (15). *Fgf*8a is equivalent to variant isoform 4 described by Crossley and Martin (7). Our third isoform, *FGF8*e, is analogous to another mouse isoform, namely variant 7 (7). This human *FGF8* isoform differs from the mouse counterpart in only 4 of 29 amino acids coded by an exon sequence not present in either *FGF8*a or *FGF8*b cDNAs. Although there is extensive homology between the known mouse and the human isoforms in the coding domain, the 3′-untranslated region of the human *FGF8* cDNAs is shown here to vary significantly from that of the mouse *Fgf8* cDNA. It is not known whether such variation may have a *cis*-acting regulatory effect on *FGF8* mRNA translation or stability in human cells and tissues compared to the mouse model.

Our interest in isolating the cDNAs from prostatic epithelial cells was prompted by the earlier characterization of the gene products in the mouse as AIGFs (4). Although it is very interesting to find expression of certain *FGF8* mRNA isoforms in prostate epithelial cells, we failed to demonstrate that androgen can induce a strong response in the expression of *FGF8* mRNAs in one test system, the androgen-responsive LNCaP cell line. Although LNCaP cells contain an androgen receptor system, the receptor gene is known to carry a single point mutation changing threonine to alanine at codon 868 in the ligand binding domain (18). There is also evidence that this abnormality of the androgen receptor affects steroid binding characteristics and response to antiandrogens (18, 19). Although *FGF8* expression is not stimulated by androgen in LNCaP cells, exposure of these cells to recombinant FGF8 protein, however, does stimulate their growth (15).

Our finding that human FGF8 isoforms have different potencies in inducing morphological transformation of NIH3T3 cells and their *in vivo* tumorigenicity is consistent with previous results with the mouse isoforms (6, 8, 9). Since the human FGF8a and FGF8b are identical in amino acid sequence to the corresponding mouse isoforms, these results further validate the previous observations. Additionally, evidence is now presented that the new isoform FGF8e also exhibits a moderate capacity to induce morphological transformation in NIH3T3 cells and to promote tumorigenicity *in vivo*. Why does one isoform display marked transforming ability whereas others do not? It may be logical to postulate that variation in biological effects of the isoforms might be related to their binding affinity to FGF receptors. In other words, the demonstrated amino-terminal differences in the human FGF8 isoforms are likely to determine which isoform or isoforms can bind to FGFRs present on NIH3T3 cells and thereby activate the signaling pathway necessary for bringing about morphological transformation. In addition to the possible receptor specificity of the isoforms (controlling the transforming potential of the isoforms), differences in affinity of each isoform for a single receptor could conceivably also affect receptor occupancy and thus the strength of the signal.

There is evidence that FGF8b and FGF8c may activate the "c" splice form of FGFR3, and FGFR4, while FGF8b is also capable of activating the c splice form of FGFR2 (5). Perhaps NIH3T3 cells express preferentially an FGFR that interacts with FGF8b but not the other isoforms. Alternatively, receptor interactions could be equal with one or more isoforms but

varied in their signaling responses. It is not possible to distinguish between these possibilities at present. The notion that differences in the amino-terminal portion of FGFs can influence their interactions with FGFRs is illustrated by the observation that FGF4 truncated at NH_2-terminus is more efficient in binding FGFR *in vitro* than the full-length FGF4 (20). On the other hand, whereas both the amino-truncated and full-length versions of FGF7 display equivalent binding to FGFR, the truncated protein, unlike full-length FGF7, fails to induce intracellular tyrosine phosphorylation (21). Therefore, to understand clearly the functional differences between FGF8 isoforms, it will first be necessary to further define isoform/FGFR interactions and then scrutinize the signals elicited by these complexes.

Finally, detection of expression of *FGF8* mRNAs in prostatic epithelial cell lines presents a rationale for asking whether expression may have a role in prostate tumorigenesis in particular, and perhaps in human malignancy in general. In this connection, it is interesting to find a recent report (22) that describes *FGF8* expression in prostate cancer. By the method of *in situ* hybridization using mouse *FGF8* antisense riboprobe, a significant up-regulation of *FGF8* expression was found in high-grade prostate tumors, whereas stroma, including endothelium of blood vessels, were negative for *FGF8* expression. It would now be important to determine whether isoform-specific expression of *FGF8* may have a role in prostate tumor growth and progression. Our isolation and characterization of three of the *FGF8* cDNA isoforms provides essential materials and information for future investigations on the biological functions of these and, potentially, other isoforms of this human growth factor in normal and abnormal proliferations.

Materials and Methods

Cell Lines. Human prostate carcinoma cell lines LNCaP, DU145, PC-3, and ALVA-31, obtained from Gary J. Miller (23), were grown in RPMI 1640 with 10% FBS, and the mouse fibroblast cell line NIH3T3 was grown in DMEM with 10% FBS. Both media were supplemented with streptomycin, penicillin, and L-glutamine. Adult human prostatic epithelial cells (MLC $SV40^-$), obtained from Johng S. Rhim (24), were grown in K-SFM (Life Technologies, Inc.) serum-free medium. All cell lines were maintained at 37° in 5% CO_2.

RT-PCR Detection of *FGF8* Expression in Prostate Carcinoma Cell Lines. Total RNA was extracted from the cells by using an RNA isolation kit (Stratagene), from which poly(A)$^+$ RNAs were isolated by oligo(dT) cellulose chromatography (25). Poly(A)$^+$ RNA (2 μg) was reverse transcribed by M-MuLV reverse transcriptase and oligo(dT)-17 primer in buffers (Life Technologies, Inc.) in a 20-μl reaction volume at 37°C for 1 h along with a negative control reaction without reverse transcriptase. Aliquots (4 μl) of reverse-transcribed products were used for PCR amplification using a primer pair specific for mouse *Fgf8* exon 5 region. The 5′ primer was RB376 (5′-AAAGGCAAGGACTGCGTCTTCACG-3′), and the 3′ primer was RB359 (5′-CGTGAAGGGCGGGTAGTTGAG-3′). Amplification was carried out in a 50-μl reaction for 35 cycles with denaturation at 94°C for 1 min, annealing at 68°C for 50 s, and extension at 72°C for 1 min 30 s. As a positive control, *GAPDH* message was amplified using a sense primer, RB146 (5′-CCACCCATGGCAAATTCCATGGCA-3′), and an antisense primer, RB147 (5′-TCTAGACGGCAGGTCAGGTCCAC-3′), under identical PCR amplification conditions. Amplified products (10 μl) were analyzed on a 2% agarose gel and DNA bands visualized by ethidium bromide staining. To determine the specificity of the products, Southern blots were analyzed either using ^{32}P-labeled mouse *Fgf8* cDNA or ^{32}P-labeled GAPDH cDNA as probe.

To detect isoform-specific mRNA expression, 2 μg of total RNA from each *FGF8* isoform-transfected NIH3T3 cell line or 2 g of poly(A)$^+$ RNA from prostate epithelial cell lines and human tissues were reversed transcribed in a 20-μl reaction volume as described above. RNAs of human tissues (adult kidney, prostate, and testes) were purchased from Clontech. Aliquots (5 μl) of reverse-transcribed products were used for PCR amplification using a primer pair. The 5′ primer, RB416 (5′-TGAGCTGCCTGCTGTTGCACTT-3′), and the 3′ primer, RB418 (5′-TGAAGACGCAGTCCTTGCCTT-3′), are positioned at 23–44 and 334–355 nucleotide positions of human FGF8a (Fig. 2). Amplification was carried out in a 50-μl reaction for 40 cycles with denaturation at 95°C for 3 min, annealing at 94°C for 1 min followed by 61°C for 30 s and 72°C for 30 s, and final extension at 72°C for 5 min. Amplified products (20 μl) were analyzed on a 3% agarose gel, and DNA bands were visualized by ethidium bromide staining. The specificity of the products were confirmed by Southern blots using an internal sequence oligonucleotide probe, RB402 (5′-TGAGCTGATCCGTCACCA-3′), located at nucleotide positions 89–106 of FGF8a (Fig. 2) and common to all isoforms. The probe was end labeled using [γ-^{32}P]ATP. This strategy yielded products of 333, 366 and 420 bp, corresponding to FGF8a, FGF8b and FGF8e RNA species, respectively, which were readily resolved under the conditions used for electrophoresis.

Molecular Cloning of *FGF8* cDNAs. A pair of oligonucleotide primers were designed based on the NH_2-terminal and COOH-terminal nucleotide sequence of the mouse *Fgf8* cDNA (4) coding sequence. These were the 5′ primer, RB202 (5′-CCATGGGCAGCCCCCGCTCCG-3′), and the 3′ primer, RB203 (5′-GCCTATCGGGGCTCCGGGGCCCAAG-3′). Poly(A)$^+$ RNAs isolated from the DU145 prostate carcinoma cell line were amplified by RT-PCR using this primer pair, the PCR products were cloned into the TA cloning vector (Invitrogen), and transformed *Escherichia coli* colonies were screened by hybridization with mouse *Fgf8* cDNA. Positive clones were selected, and the plasmids were extracted and sequenced by Sanger's (26) dideoxy chain termination method. A series of oligonucleotides (20–24-mers) were synthesized from positions every 200 bases along the coding sequence and used as primers for sequencing. The two ends of the cDNAs were sequenced using oligonucleotide primers corresponding to the T7 promoter and M13 reverse sequences present in the plasmid vector. DNA sequences were aligned using the GENALIGN (Intelligenetics) program on a SUN microcomputer. This analysis resulted in isolation and identification of three different human *FGF8* cDNA clones with varied sequences at the 5′ end of the coding region.

Cloning of 3′-Untranslated Region by RACE. Poly(A)$^+$ RNA from DU145 cells was used in a reaction carried out with 3′-Amplifier RACE Kit (Clontech). The first cDNA was synthesized using NN-1-oligo(dT) CDS primer, followed by PCR amplification with RB168 primer (5′AAGGCAAGGACTGCGTATTCACAG-3′) and anchor primer in 25 cycles of 94°C for 45 s, 60°C for 45 s, and 72°C for 2 min (primary PCR). RB250 primer (5′-GCTTCGAGTTCCTCAACTAC-3′) and anchor primer were then used for secondary or nested PCR (25 cycles) under the same conditions. A 350-bp amplified product was obtained by this procedure. After cloning into the TA cloning vector, the sequence of the insert was determined.

Expression of FGF8 in Eukaryotic Cells. All three isoforms of *FGF8* cDNAs (8a, 8b, and 8e) were excised from the TA vector by *Eco*RI digestion and cloned into the corresponding site of the eukaryotic expression vector pcDNA3 (Invitrogen) in both the sense and antisense orientations. Plasmids were transfected into NIH3T3 cells either by calcium phosphate method as described previously (27) or by LipofectAMINE (Life Technologies, Inc.) as per the manufacturer's instructions. Twenty-four h after transfection, the cells were transferred to new plates, and the cells were selected for stable transfectants with DMEM-10% FBS containing 400 μg/ml G418 (Geneticin, Life Technologies, Inc.). These cells were grown for 7–10 days. At least 60 colonies were pooled from each transfection to generate the stable cell lines used in the transformation and tumorigenicity assays. Supernatant fluids from the transfected and selected cell cultures were collected to determine their effect on inducing morphological transformation of NIH3T3 cells. For the latter work, vector-transfected NIH3T3 cells rather than untransfected NIH3T3 cells were used since the conditioned medium contained G418.

Northern Blot Analyses. Total RNA was isolated by the acid guanidinium thiocyanate method (28). The samples were separated by electrophoresis on a 1% denaturing formaldehyde agarose gel, and transferred to Hybond N membrane (Amersham Corp.). The hybridization procedure for Northern blots of human mRNAs obtained from Clontech was as specified by the company. The blots were hybridized to a ^{32}P-labeled

FGF8 cDNA probe. After exposure to X-ray film, the filters were stripped and rehybridized to a control human β-actin probe for normalization of the amount of RNA loaded.

Stimulation of LNCaP Cells by Androgen and Examination of *FGF8* Expression. LNCaP cells were grown in 10% serum-supplemented RPMI until approximately 75% confluency was attained. After the medium was removed, the cells were washed gently on the plate three times with PBS. RPMI containing 5% charcoal-stripped serum was placed on the cells that were then allowed to sit for 72 h. Androgen (dihydrotestosterone) was added at 10^{-8} M to fresh medium (RPMI plus 5% charcoal-stripped serum), and the cells were incubated with this medium. Cells collected at different time intervals were used to extract total RNA. Contaminating DNA from the RNA preparations was removed by DNase I digestion according to the Clontech protocol. *FGF8* expression was detected by RT-PCR as described above. Equal amounts of RT products were also subjected to GAPDH amplification to verify proportions of the starting materials.

Tumorigenicity Studies. Tumorigenicity was examined by inoculation of cells into the anterior chamber of the eyes of 5-week-old nude mice. The mice were anesthetized with 40 mg/kg of pentobarbital delivered i.p., and then approximately 10^2-10^4 cells in suspension were injected only into the left eye as described previously (16, 17). In the first experiment, three mice were injected for each cell line at each cell concentration, and the animals were observed for a period of 4 weeks. In the repeat experiment, again three mice were used for each cell concentration, but the observation period was extended to 11 weeks. The formation of tumors was monitored every other day under the microscope. The experimental animals were cared for in accordance with institutional guidelines, and they were sacrificed soon after the tumor development.

Accession Numbers. The nucleotide sequence data reported in this paper can be retrieved from the GenBank under the following accession numbers: U46211, *FGF8a*; U46212, *FGF8b*; U46213, *FGF8e*; and U46214, *FGF8* 3′-untranslated region.

Acknowledgments

We thank N. Rudra-Ganguly and K. Moffat for assistance with parts of this work, Y-K. T. Fung for advice and help with the *in vivo* tumorigenesis work, J. S. Rhim for MLC SV40$^-$ cells, and L. Sanchez and F. Miyagawa for manuscript preparation.

References

1. Basilico, C., and Moscatelli, D. The FGF family of growth factors and oncogenes. Adv. Cancer Res., *59:* 115–165, 1992.

2. Johnson, D. E., and Williams, L. T. Structural and functional diversity in the FGF receptor multigene family. Adv. Cancer Res., *60:* 1–41, 1993.

3. Mason, I. J. The ins and outs of fibroblast growth factors. Cell, *78:* 546–552, 1994.

4. Tanaka, A., Miyamoto, K., Minamino, N., Takeda, M., Sato, B., Matsuo, H., and Matsumoto, K. Cloning and characterization of an androgen-induced growth factor essential for the androgen-dependent growth of mouse mammary carcinoma cells. Proc. Natl. Acad. Sci. USA, *89:* 8928–8932, 1992.

5. MacArthur, C. A., Lawshé, A., Xu, J., Santos-Ocampo, S., Heikinheimo, M., Chellaiah, A. T., and Ornitz, D. M. FGF-8 isoforms activate receptor splice forms that are expressed in mesenchymal regions of mouse development. Development (Camb.), *121:* 3603–3613, 1995.

6. MacArthur, C. A., Shankar, D. B., and Shackleford, G. M. FGF-8, activated by proviral insertion. cooperates with the *Wnt-1* transgene in murine mammary tumorigenesis. J. Virol., *69:* 2501–2507, 1995.

7. Crossley, P. H., and Martin, G. R. The mouse *Fgf8* gene encodes a family of polypeptides and is expressed in regions that direct outgrowth and patterning in the developing embryo. Development (Camb.), *121:* 439–451, 1995.

8. Kouhara, H., Koga, M., Kasayama, S., Tanaka, A., Kishimoto, T., and Sato, B. Transforming activity of a newly cloned androgen-induced growth factor. Oncogene, *9:* 455–462, 1994.

9. MacArthur, C. A., Lawshé, A., Shankar, D. B., Heikinheimo, M., and Shackleford, G. M. FGF-8 isoforms differ in NIH3T3 cell transforming potential. Cell Growth & Differ., *6:* 817–825, 1995.

10. Lorenzi, M. V., Long, J. E., Miki, T., and Aaronson, S. A. Expression cloning, developmental expression and chromosomal localization of fibroblast growth factor-8. Oncogene, *10:* 2051–2055, 1995.

11. Catalona, W. J. Drug therapy: management of cancer of the prostate. N. Engl. J. Med., *331:* 996-1004, 1994.

12. Isaacs, J. T., Lundmo, P. I., Berges, R., Martikainen, P., Kyprianou, N., and English, H. F. Androgen regulation of programmed death of normal and malignant prostatic cells. J. Androl., *13:* 457–464, 1992.

13. Isaacs, W. B., Bova, G. S., Morton, R. A., Bussemakers, M. J. G., Brooks, J. D., and Ewing, C. M. Molecular biology of prostate cancer. Semin. Oncol., *21:* 514–521, 1994.

14. Crawford, E. D., Eisenberger, M. A., McLeod, D. C., Spaulding, J., Benson, R., Dorr, F. A., Blumenstein, B. A., Davis, M. A., and Goodman, P. J. A control randomized trial of Leuprolide with and without flutamide in prostate cancer. N. Engl. J. Med., *321:* 419–424, 1989.

15. Tanaka, A., Miyamoto, K., Matsuo, H., Matsumoto, K., and Yoshida, H. Human androgen-induced growth factor in prostate and breast cancer cells: its molecular cloning and growth properties. FEBS Lett., *363:* 226–230, 1995.

16. Xu, H-J., Sumaji, J., Hu, S. X., Banerjee, A., Uzvolgyi, E., Klein, G., and Benedict, W. F. Intraocular tumor formation of Rb reconstituted retinoblastoma cells. Cancer Res., *51:* 4481–4485, 1991.

17. Fung, Y-K., T'Ang, A., Murphee, A. L., Zhang, F-H., Qiu, W-R., Wang, S-W., Shi, X-H., Lee, L., Driscoll, B., and Wu, K-J. The *Rb* gene suppresses the growth of normal cells. Oncogene, *8:* 2659–2672, 1993.

18. Veldscholte, J., Ris-Stalpers, C., Kuiper, G. G., Jenster, G., Berrevoets, C., Claassen, E., van Rooij, H. C., Trapman, J., Brinkmann, A. O., and Mulder, E. A mutation in the ligand binding domain of the androgen receptor of human LNCaP cells affects steroid binding characteristics and response to anti-androgens. Biochem. Biophys. Res. Commun., *173:* 534–540, 1990.

19. Berrevoets, C. A., Veldschotte, J., and Mulder, E. Effects of antiandrogens on transformation and transcription activation of wild-type and mutated (LNCaP) androgen receptors. J. Steroid Biochem. Mol. Biol., *46:* 731–736, 1993.

20. Bellosta, P., Talarico, D., Rogers, D., and Basilico, C. Cleavage of K-FGF produces a truncated molecule with increased biological activity and receptor binding affinity. J. Cell Biol., *121:* 705–713, 1993.

21. Ron, D., Bottaro, D. P., Finch, P. W., Morris, D., Rubin, J. S., and Aaronson, S. A. Expression of biologically active recombinant keratinocyte growth factor. J. Biol. Chem., *268:* 2984–2988, 1993.

22. Leung, H. Y., Dickson, C., Robson, C. N., and Neal, D. E. Overexpression of fibroblast growth factor-8 in human prostate cancer. Oncogene, *12:* 1833–1835, 1996.

23. Miller, G. J., Stapleton, G. E., Hedlund, T. E., and Moffat, K. A. Vitamin D receptor expression, 24-hydroxylase activity, and inhibition of growth by 1α, 25-diydroxyvitamin D3 in seven human prostatic carcinoma cell lines. Clin. Cancer Res., *1:* 997–1003, 1995.

24. Lee, M-S., Garkovenko, E., Yun, J. S., Weijerman, P. C., Peehl, D. M., Chen, L-S., and Rhim, J. S. Characterization of adult human prostatic cells immortalized by polybrene-induced DNA transfection with a plasmid containing an origin-defective SV40 genome. Int. J. Oncol., *4:* 821–830, 1994.

25. Aviv, H., and Leder, P. Purification of biologically active globin messenger RNA by chromatography on oligothymidylic acid-cellulose. Proc. Natl. Acad. Sci. USA, *69:* 1408–1412, 1973.

26. Sanger, F., Coulson, A. R., Barrell, B. G., Smith, A. J. H., and Roe, B. A. Cloning in single-stranded bacteriophage as an aid to rapid DNA sequencing. J. Mol. Biol., *143:* 161–178, 1980.

27. Ghosh, A. K., and Roy-Burman, P. Characterization of enhancer elements and their mutations in the long terminal repeat of feline endogenous RD-114 proviruses. J. Virol., *63:* 4234–4241.

28. Chomczynski, P., and Sacchi, N. Single-step method of RNA isolation by acid guanidinium thiocyanate-phenol-chloroform extraction. Anal. Biochem., *162:* 156–159, 1987.